MAPPING CHLOROPHYLL IN THE AMAZON FLOODPLAIN LAKES WITH MERIS IMAGES

Cláudio Clemente Faria Barbosa [(1)], Lino Augusto Sander[(1)], Evlyn M. L. M Novo[(1)].

(1) National Institute of Spatial Research (INPE), Av. dos Astronautas, 1758, Jd. Da Granja, São José dos Campos, Zip code: 12227-010, Brazil, Email: claudio@dpi.inpe.br, lino@dsr.inpe.br, evlyn@dsr.inpe.br

ABSTRACT

The aim of this research was to develop models based on MERIS images for estimating the spatial distribution of chl-a concentration in lakes of complex and turbid waters of Amazon basin floodplain.
In situ measurements taken before, simultaneously and after MERIS images acquisition, were used to fit two and three spectral band models. Three approaches were conducted to assess the estimate chlorophyll-a concentration: a) An iterative computational search method to find the best wavelengths set based in situ data (spectra and *chl-a* concentration) resulted R^2 of 0.91 for two bands model and R^2 of 0.95 for three bands. b) The same iterative search applied to MERIS bands simulated from *in situ* spectra resulted R^2 of 0.87 for two bands and R^2 of 0.94 of for three bands; c) Models from the second approach applied to c*hl-a* concentration of stations sampled on the day of the image acquisition resulted R^2 of 0.77 for the two bands model and R^2 0.75 of for the three bands.

1. INTRODUCTION

The Amazon drainage basin is one of the most important river systems in the world covering approximately 6.5 x 106 km^2, of which around 17% are wetlands (Hess *et al.*, 2003; Junk, 1997). The main stem floodplain in central Amazonia has approximately 300 x 10^3 km^2 (Junk and Weber, 1996; Melack, 1984), with 8050 lakes (Melack, 1984; Sippel *et al.*, 1992). The primary productivity of these lakes, whose dynamic is affected by both land use and the flood pulse, has been the subject of several studies (Costa, 2005; Engle *et al.*, 2008). Many of these floodable areas are remote, inaccessible and formed by large lakes, making remote sensing a feasible tool for their study and monitoring. The photosynthetic pigment chlorophyll-a (*chl-a*) is a key indicator of primary productivity and it causes changes in water color that can be registered by remote sensors and transformed into useful information. In this context, the aim of this research was to estimate *chl-a* concentration in lakes of complex and turbid waters of a large Amazon basin floodplain using MERIS/Envisat images and empirical models. In situ measurements (spectroradiometric and limnological) taken before, simultaneously and after MERIS/Envisat image acquisition were used to fit two and three bands empirical models (Dall'Olmo & Gitelson, 2005).

2. MATERIALS AND METHODS

2.1. Study area

The Lago Grande de Curuai (LGC) floodplain, located along the Amazon River near Óbidos city (Brazil), 900 km upstream from the Atlantic Ocean (Fig. 1-a), is a complex system of about 30 shallow interconnected lakes linked to the Amazon River by several channels including open water, flooded savannas and floating grasses. The dynamics of flooding in LGC is related to the seasonal fluctuation of Amazon River, having an annual monomodal pattern (Fig. 1-b) (Junk et al., 1989). The seasonal fluctuations in the water level vary from approximately 5 up to 7 meters. During the rising water stage, Amazon River water flows into the floodplain enlarging the lake area from 700 km^2 to 1600 km^2 (Barbosa, 2005). These flooding dynamics can be characterized by four stages: rising, high, receding and low water. Rising and receding stages are characterized by maximum changes in water level and low and high stages are characterized by minimum changes in water level (Barbosa, 2005). The floodplain of LGC was selected because it is suitable for monitoring with medium resolution sensors such as MERIS. Moreover, this floodplain area has been subjected to intense human impact during the 20th century and has already presented signs of anthropogenic eutrophication (Affonso et al., 2011).

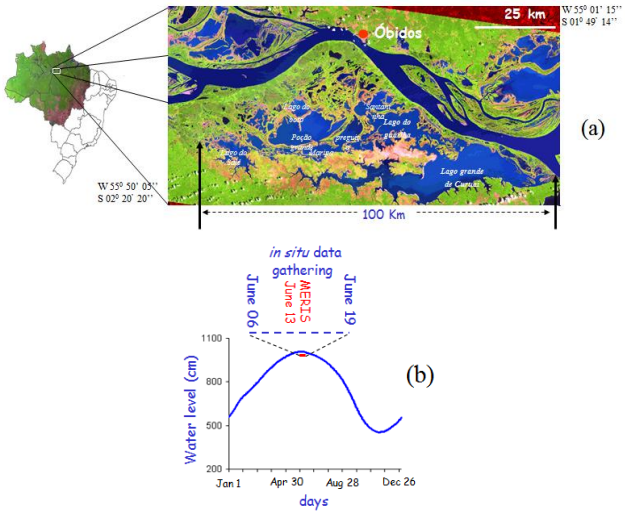

Figure 1- (a) Location of Lago Grande de Curuai (LGC) illustrated by Landsat Thematic Mapper (TM) images. (b) Annual hydrographs at LGC (Data from the Brazilian Water Agency - ANA).

2.2. In situ data collection and MERIS images

The field campaign was carried out from June 6 to June 19, 2004, during the high water stage, condition of minimal change in the water level (Fig. 1-b), for acquiring *in situ* measurements (spectroradiometric and limnological). Water samples for analytical determination of optically-active constituents concentrations (chlorophyll, total suspended solids and dissolved organic matter) were collected simultaneously with spectroradiometric measurements. Field spectra (Fig. 2-a) were measured with a Spectron Model SE-590 spectroradiometer, with a 6° field-of-view, a meter above the water and instantaneous field of view (IFOV) of 0.05 m^2. A white Spectralon reflectance standard panel (Labsphere, Inc North Sutton, NH) was used as white reference panel. The measurements were taken between 10 AM to 2 PM, with azimuth angles of 90° with respect to the sun plane, and with nadir viewing angle of 40° to minimize sun glint. Two water-leaving radiance spectra $L_w(\lambda)$ were obtained for each sampling station, each one as an average of four successive readings of the spectroradiometer. For each $L_w(\lambda)$, the radiance reflected, in the same viewing angle, by a white reference panel $L_{ref}(\lambda)$ was taken, also as an average of four successive readings. $L_w(\lambda)$ and $L_{ref}(\lambda)$ were used to derive the bi-directional reflectance factor (BRF).

Seventy two water samples were collected integrating the water column from surface to Secchi disk depth. The samples were kept at cool temperatures and filtered on the same day through Whatman type GF/F glass-fiber filters and frozen for analytical measures of *ch-a*, Total suspended solids (TSS) and dissolved organic and inorganic carbon (DOC/DIC). TSS was determined based on Wetzel and Likens (1991) and chlorophyll analyses were based on Nush (1980). Spectroradiometric measurements (Fig. 2-a), Secchi disk depth, turbidity and pH were taken at the same 72 water sampling stations. Turbidity and pH were taken with a Horiba sensor, calibrated every day, with reference patterns provided by the company.

The MERIS image, full resolution mode, was acquired on June 13th, 2004. Fig. 2-b shows both a color composite of MERIS image and the location of the *in situ* sampling stations (red dot), and Tab. 1 list the descriptive statistics of the Water Quality Parameters collected during the field campaign.

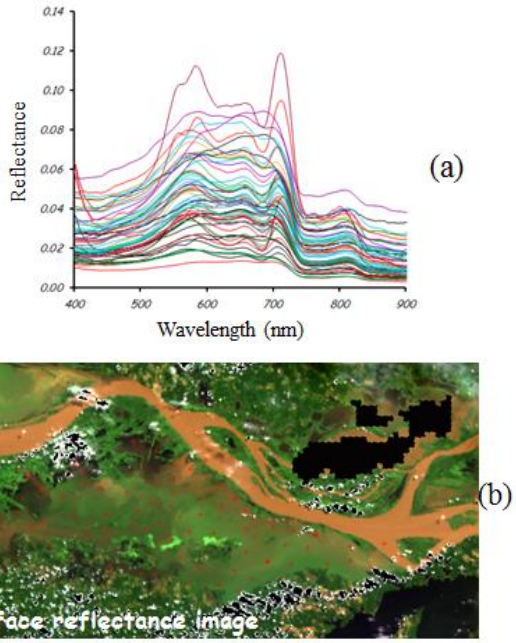

Figure 2 – (a) Bi-directional reflectance factor spectra (400–900 nm) collected during field campaign. (b) MERIS image, full resolution mode acquired on June 13th, 2004. Red dots are the location of sampling stations.

Table 1 - Descriptive Statistics of the Water Quality Parameters collected (Min- minimum, Max – Maximum, CV- coefficient of variation, N=sample size)

Water Quality Parameters — Descriptive Statistics					
	Min	Max	Average	CV	N
Chl-a (µg/L)	1.16	131.3	28.8	0.75	72
TSS (mg/L)	5.68	34.90	14.5	0.29	72
DOC (mg/L)	4.4	15.30	6.7	0.28	72
Turbidity(NTU)	5	90	30	0.40	72

2.3. Data processing

Two processing were conducted: a) MERIS image was submitted to atmosphere correction; and b) *in situ*

spectra were resampled to 15 MERIS spectral bands to simulate MERIS/Envisat data (hereinafter referred to as SimMERIS).

The MERIS image, Level 1 product, was atmospherically corrected and converted to surface reflectance using the simplified methods for atmospheric correction processor SMAC provided by ESA in the Basic ERS & Envisat (A) ATSR and MERIS Toolbox (BEAM). SMAC (Rahman & Dedieu, 1994) is a semi-empirical approximation of the radioactive transfer in the atmosphere, which calculates surface reflectance from satellite measurements. Surface reflectance at each sample station was extracted from the MERIS image for all spectral bands (MERIS image spectra).

The first step to obtain the SimMERIS spectra was to compute the bi-directional reflectance factor (BRF) spectrum at each sampling station. The BRF was computed dividing water-leaving radiance spectra $L_w(\lambda)$ by a white reference panel radiance $L_{ref}(\lambda)$. From now on, throughout the text, the BRF will be referenced as reflectance. Then, all *in situ* reflectance spectra were resampled to spectral bands of MERIS, based on MERIS Spectral Model available on: (http://earth.esa.int/pub/ESA_DOC/MERIS_Wavelengths_and_Irradiances_Model2004.xls) The difference in spatial resolution between MERIS and in situ spectra was not taken into account in this MERIS bands simulation process.

3. Data analysis and results

The data analysis consisted of: a) Qualitative comparison of spectral shape (MERIS and *in situ*); b) Fitting models for mapping chlorophyll.

3.1. Qualitative comparison of spectral shape

Fig. 3 shows together some of *in situ* reflectance spectra and spectra extracted from the MERIS image acquired concurrently during field campaign, on June 13th, 2004. Note that, with the exception of the intensity, the overall shape of spectra are very similar and their main spectral features can be visually identified, even for *in situ* spectra not measured on the day of image acquisition. Intensity differences can be explained by the uncertainty introduced by atmospheric correction, time of each measurement (lag time), difference in spatial resolution and also by the variability inherent to *in situ* radiometric data acquisition (Pereira Filho, 2005). This comparison also highlights that MERIS band positioning matches almost perfectly the diagnostic spectral features of optically active components present in inland aquatic systems, case II water (IOCCG, 2000). A correlation analysis among all *in situ* spectra acquired during the field campaign and those extracted from MERIS image (Barbosa et al. 2009) showed that on the day of image acquisition, the average correlation was 0.98, with a maximum of 0.99 and a minimum of 0.97. The average correlation for time lag ranging from 1 to 6 days (before and after the satellite overpass) varied from 0.54 to 0.95.

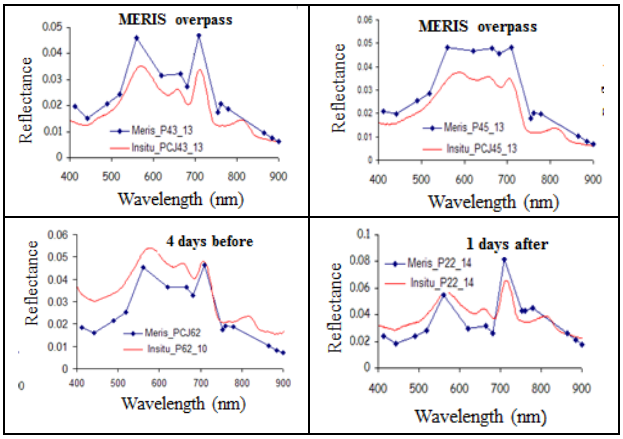

Figure 3 – *In situ* spectra (red) acquired during the field campaign and spectra extracted from MERIS image (Blue), after atmosferic correction.

3.2. Fitting models for mapping chlorophyll

Three approaches were conducted to estimate the spatial distribution of *chl-a* in the lakes of the Amazon floodplain.

1 – An iterative computational search method to find the best wavelengths set based in situ data (spectra and chl-a concentration) to input two and three spectral bands empirical models.

2 – The iterative computational search method was applied using simulated spectra (SimMERIS) to find the best MERIS bands for fitting two and three bands models for the available in situ data.

3 – *Chl-a* concentration of stations sampled on the day of the image acquisition and MERIS image, were used as input for models fitted on the second approach.

Fig. 4 shows the results of these approaches for three bands models, and Table 2 list the determination coefficients (R^2) and the best spectral bands for both, two and three band models.

The models based on *in situ* data, first approach (Fig. 4-a), explain 95% (R^2=0.95) of the *chl-a* variability in the floodplain for the three bands model against 91% for the two bands model (Tab. 2). The best bands were: λ_1= 676 nm, λ_2= 708 nm λ_3 = 774 nm for three bands model, and λ_1=723 nm λ_2=673 nm for two bands model.

The models based on simulated MERIS bands (Fig-b), explain 94% (R^2=0.94) of the *chl-a* variability for the three bands model against 87% for the two bands model (Tab. 2). The best MERIS bands were: λ_1 = band 8, λ_2 = band 9 and λ_3 = band 12 for three bands model, and λ_1= band 9, λ_2 = band 8 for two bands model.

In the third approach, when models were based on MERIS image acquired concurrently with one of the

days of the field Campaign (six sample station) and the models fitted in second approach (Figure 4-c), the model explain 86% of the *chl-a* variability for the three bands model against 80% for the two bands model (Tab. 2). Many factors such as uncertainty introduced by atmospheric correction in the image, differences in spatial resolution, and variability inherent to *in situ* acquisition process are responsible for differences between models of the approaches 2 and 3.

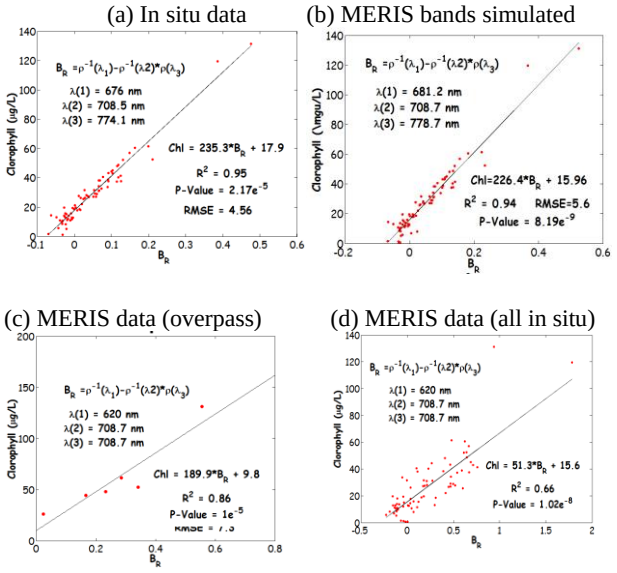

Figure 4 – Results of three bands model. (a) Based on *in situ* spectra. (b) Based on MERIS bands simulated. (c) Based on MERIS image and *chl-a* concentration of the day of sensor overpass. (d) Based on MERIS image and all *chl-a* concentration of all sampling station of the field campaign.

Table 2 – Best spectral bands and determination coefficients for two and three bands models

Input to model	Three bands		two bands	
	R^2	bands (nm)	R^2	bands (nm)
In situ spectra, tuned to best wavelengths	0.95	676 708 774	0.91	723 673
MERIS bands simulated	0.95	B8 B9 B12	0.87	B9 B8
Bands extracted from image	0.86	B8 B9 B12	0.80	B9 B8
Chl-a concentration of all sampling station	0.66	B8 B9 B12	0.66	B9 B8

Fig. 5 shows the spatial distribution of *chl-a* in the floodplain when three bands model, resulting from the third approach, was applied to MERIS image.

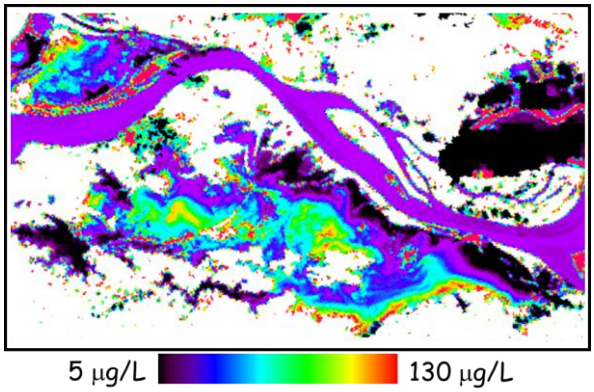

Figure 5 – Chlorophyll-a map for study area based on the three bands model fitted to the day of sensor overpass.

An attempt to use *chl-a* concentration collected in all sampling stations throughout the field campaign and MERIS image was made, but the accuracy of the model was low (Fig. 4-d). These results were already expected considering the low correlation mentioned above for up to six days lag between image acquisition and sampling stations. Changes in the optical properties of aquatic system, induced by winds, probably explain this result.

4. CONCLUSION

The results indicate that spectral bands and spatial resolution of MERIS were suitable for mapping chlorophyll in turbid water lakes along the Amazon basin. The 300 meters spatial resolution of MERIS sensor is not a constraint for its application in large lakes of the Amazon floodplain. A qualitative comparison between simulated MERIS spectra with those extracted from image suggests that: Atmospheric correction, footprint differences (0.05 m^2 against 300 m^2) between *in situ* and the MERIS sensor and time lag between *in situ* and satellite data acquisitions, were responsible for the decrease in the models accuracy. Considering that the features of Sentinel-3 are similar to MERIS, these results also demonstrate that Sentinel-3 will be suitable for mapping chlorophyll in lakes of the Amazon floodplain.

The accuracy of the MERIS image model, however, was not as high as SimMERIS, not only because of the time lag, but also because *in situ* reflectances fail to capture patchiness of phytoplankton, which can occur with different patterns and length scales depending on the underlying physical mechanisms that affect their evolution (Hillmer et al., 2008). The *in situ* spectral measurements and water samples were collected at the same 0.05 m^2 spectrometer foot print, against a pixel integrating an area of 90 x 10^3 m^2 for MERIS. The results indicate that in spite of the 300 by 300 m

resolution of MERIS and Sentinel-3 sensors, they can be efficiently applied to estimate *chl-a* concentration in Amazon floodplain lakes, case II waters. Based on the results, it can also be inferred that MERIS/Sentinel-3 images are better than the accuracy here assessed since the in situ data was not fit to represent within pixel variability.

Acknowledgements
The authors thank FAPESP (Fundação de Amparo à Pesquisa do Estado de São Paulo) for funding all field campaigns (Process 2003/06999-8) and ESA for MERIS image through the project ID #10990.

5. REFERENCES

1. Affonso, A. G., Barbosa, C. C. F., & Novo, E. M. L. M. (2011). Water quality changes in floodplain lakes as a function of the Amazon River flood pulse: Lago Grande de Curuaí (Pará). Brazilian Journal of Biology, 71 (3).

2. Barbosa, C. C. F. (2005). Sensoriamento remoto da dinâmica de circulação da água do sistema planície de Curuaí/Rio Amazonas. PhD Thesis, National Institute for Space Research (INPE), São José dos Campos, Brazil (http://mtc-m18.sid.inpe.br/col/sid.inpe.br/MTC-m13@80/2006/02.22.15.03/doc/publicacao.pdf).

3. Barbosa, C. C. F.; NOVO, E. M. M. Remote sensing of the water properties of the Amazon floodplain lakes: the time delay effects between in-situ and satellite data acquisition on model accuracy. In: International Symposium on Remote Sensing of Environment: Sustaining the Millennium Development Goals, 33, 2009, Stressa.

4. Costa, M. P. F. (2005). Estimate of net primary productivity of aquatic vegetation of the Amazon floodplain using Radarsat and JERS-1. International Journal of Remote Sensing 26, 4527–4536.

5. Dall'Olmo, G., & Gitelson, A. A. (2005). Effect of bio-optical parameter variability on the remote estimation of chlorophyll-a concentration in turbid productive waters: experimental results. Appl. Opt., 44, 412-422.

6. Engle, D. L., Melack, J. M., Doyle, R. D., & Fisher, T. R. (2008). High rates of net primary production and turnover of floating grasses on the Amazon floodplain: implications for aquatic respiration and regional CO2 flux. Global Change Biology, 14, 369–381.

7. Hess, L. L., Melack, J. M., Novo, E. M. L. M., Barbosa, C.C.F., & Gastil, M. (2003). Dual-seasonal mapping of wetland inundation and vegetation for the Central Amazon Basin. Remote Sensing of Environment, 87, 404–428.

8. Hillmer, I. A., Van Reenen, P. Imberger, J., & Zohary, T. (2008). Phytoplankton patchiness and their role in the modeled productivity of a large, seasonally stratified lake. Ecol. Model, 218, 49-59.

9. IOCCG (2000). Remote sensing of ocean colour in coastal and other optically-complex waters. In S. Sathyendranath, Reports of the International Ocean Colour Coordinating Group, No. 3, IOCCG, Dartmouth, Canada.

10. Junk, W. S., & Weber, G. E. (1996). Amazonian floodplains: A limnological perspective. Verth International Review Limnology, 26, 149-157.

11. Melack, J. M. (1984). Amazon floodplain lakes: Shape, fetch, and stratification. Verth. International Verein. Limnology, 22, 1278-1282.

12. Nush, E. A. (1980). Comparison of different methods for chlorophyll and phaeopigment determination. Arch. Hydrobiol. Beih. (14-39). Stuttgart.

13. Pereira Filho, W., Barbosa, C. C. F., & Novo, E. M. L. M. (2005). Influência das condições do tempo em espectros de refletância da água. In: SIMPÓSIO BRASILEIRO DE SENSORIAMENTO REMOTO, 12 Goiânia. Anais São José dos Campos: INPE. 415-422.

14. Rahman, H., & Dedieu, G., (1994). SMAC: A simplified method for the atmospheric correction of satellite measurements in the solar spectrum. International Journal of Remote Sensing, 15 (1), 123-143.

15. Sippel, S. J., Hamilton, S. K., & Melack, J. M. (1992). Inundation area and morphometry of lakes on the Amazon River floodplain, Brazil, Arch. Hydrobiol, 123, 385-400.

16. Wetzel, R. G., & Likens, G. E. (1991). Limnological Analyses, 2nd Ed., Springer-Verlag, New York.